

PH570 Course Project

Optical Investigation of Shape and Size-controlled Silver Nanoparticles

Utkarsh (190260044)
Sanyam Singhal (19D170028)

October 31, 2023

Contents

1	Introduction	2
2	Localized Surface Plasmons and Mie Theory: Theoretical Background	2
3	Silver Nanoparticle Synthesis: The Polyol Method	4
3.1	Literature Review	4
3.2	Our Synthesis	4
4	Characterization Techniques and Observations	6
4.1	Transmission electron microscopy	6
4.1.1	Size Distribution of Ag particles	7
4.2	Selected area electron diffraction	8
4.3	UV-Vis Absorption Spectroscopy	9
4.4	Fourier Transform Infrared Spectroscopy	10
5	Mie Theory Analysis	11
6	Conclusion	12
7	References	12

1 Introduction

Silver (Ag) metal possesses the highest electrical/thermal conductivity and reflectivity among other metals (Au/Pt/Pd). The phenomenon, known as Localized Surface Plasmon Resonance (LSPR) [1], in Ag nanoparticles (NPs) is mainly responsible for their successful utilization in bio-sensors, composite fibers, cryogenic superconductors, and in cosmetics [2]. Plasmonic behavior in noble metals is highly controlled by factors like their shape, size, and dielectric of the surrounding media. Herein, we controlled the size of Ag NPs using the Polyol method [3, 4]. In this method, a solid inorganic precursor (AgNO₃) is suspended into a liquid polyol such as ethylene glycol, diethylene glycol, or a mixture of both. The mixture is magnetically stirred and heated at an appropriate temperature to reach the boiling point of polyol. This results in the reduction of the compound, which yields metal NPs. A capping reagent (such as poly N-vinyl pyrrolidone, PVP) is used to prevent the agglomeration of NPs. The surface plasmon absorption in Ag NPs has been characterized using UV/vis spectroscopy. The number of peaks obtained in absorption studies is related to the way the particles get polarized, which in turn, is determined by the symmetry of nanoparticles [5]. A spherical particle which is the most symmetrical shape has extinction spectra with just one peak because a small sphere can be polarized only in dipole mode. On the other hand, the presence of two peaks (non-spherical symmetry) shows the particles could be polarized both in dipole as well as quadrupole modes. We further incorporated Mie's theory to find the dielectric constant of the surrounding media [2]. We also imaged the nanoparticles using Transmission Electron Microscopy, also performing Selected area electron diffraction in the same setup to get a good estimate of the miller indices of the planes present in our nanoparticles. In the end, we also performed Fourier transform infrared spectroscopy to analyze the bonding between the PVP and Silver atoms in the nanoparticle.

2 Localized Surface Plasmons and Mie Theory: Theoretical Background

Mie was the first to describe the plasmon resonance quantitatively by solving Maxwell's equations with the appropriate boundary conditions for spherical particles. It is the only simple and exact solution to Maxwell's equations that is relevant to spherical and well-separated particles. Moreover, most of the preparation techniques yield particles that are approximately spherical in shape. This leads to results that can be modeled reasonably well using this theory. For nanoparticles whose size regime is very much smaller than the wavelength of the exciting source of light, it is assumed that only the dipole absorption of the Mie equation contributes to the extinction cross section of the nanoparticles. The extinction cross section represents loss of energy from the incident electromagnetic wave due to both scattering and absorption. The Mie scattering theory then reduces to the following form:

$$C_{\text{ext}} = \frac{24\pi^2 R^3}{\lambda} \varepsilon_m^{\frac{3}{2}} \frac{\varepsilon_2}{(\varepsilon_1 + 2\varepsilon_m)^2 + \varepsilon_2^2} \quad (1)$$

Here C_{ext} is the extinction cross section for the nanoparticles dispersed in a medium, R is the radius of the particle, λ is the wavelength of the electromagnetic wave and $\epsilon = \epsilon_1 + i\epsilon_2$ is the complex dielectric function of the metal particle embedded in the surrounding matrix with a dielectric constant ϵ_m . Within the dipole approximation there is no size dependence except for varying intensity. Experimentally, however, one observes a strong size dependence on the plasmon bandwidth and peak position. Researchers have observed the SPR band shifts to both higher and lower energies for decreasing particle dimensions. For silver nanoparticles classical conductivity models predict redshifts due to the increased damping of the electron motion with decreasing size [14][15]. However, blueshifts because of quantum size effects have also been observed [16].

The intense absorption band at around 410 nm is due to the collective oscillation of all free electrons in the silver particles resulting from the interaction with electromagnetic radiation. The electric field of the incoming radiation induces the formation of a dipole in the nanoparticle. A restoring force in the nanoparticle tries to compensate for this, resulting in a specific resonance wavelength. The strength and frequency of this resonance is related to the total number of electrons in the oscillating dipole (defined essentially by the particle volume or R^3), the complex dielectric function $\epsilon(\omega)$ and the dielectric constant of the local medium ϵ_m .

The dipolar plasmon response of the nanoparticles is often defined by its polarizability, which can be expressed in terms of the above-mentioned parameters by the equation

$$\alpha = 4\pi\varepsilon_0 R^3 \frac{(\varepsilon - \varepsilon_m)}{(\varepsilon + 2\varepsilon_m)} \quad (2)$$

Here ϵ is the wavelength-dependent dielectric functions of the material comprising the particle.

The resonance condition leading to maximum polarization is $\epsilon + 2\epsilon_m = 0$, requiring $\epsilon(\omega)$ to be negative. However, the complex dielectric function may be divided into real and imaginary components $\epsilon_1(\omega)$ and $\epsilon_2(\omega)$ in order to remove the phase-dependent term from the equation; resonance is thus achieved when $\epsilon_1(\omega) = -2\epsilon_m$ and $\epsilon_2(\omega) \ll 1$. The dielectric function is negative when ω is below some threshold frequency ω_p , known also as the plasma frequency. The relationship between $\epsilon(\omega)$ and ω_p can be illustrated by the Drude model, a conceptually useful description of free-electron behavior in metals. Here $\epsilon_1(\omega)$ and $\epsilon_2(\omega)$ can be approximated in terms of ω_p and γ , the plasma relaxation frequency:

$$\epsilon = \epsilon_1 + i\epsilon_2 = 1 - \frac{\omega_p^2}{\omega^2 + \gamma^2} + i\frac{\omega^2\gamma}{\omega(\omega^2 + \gamma^2)}.$$

with

$$\omega = 2\pi\frac{c}{\lambda} \quad \text{and} \quad \gamma = \frac{V_f}{L}.$$

Here V_f is the Fermi velocity of the electrons, L is the mean free path length in the bulk material and c is the velocity of light.

For metal particles with radius R smaller than the mean free path L of conduction electrons in the bulk metal, the mean free path can be dominated by collisions with the particle boundary. Thus the damping constant (γ) in Drude theory, which is the inverse of the collision time for conduction electrons, is increased because of additional collisions with the boundary of the particle [17]. Under the assumption electrons are diffusely reflected at the boundary, γ can be written as

$$\gamma = \frac{V_f}{L} + \frac{V_f}{R}.$$

For silver nanoparticles we have used the values of $V_f = 1.38 \times 10^6 \text{ m s}^{-1}$, $L = 57 \text{ nm}$ and $\omega_p = 1.39 \times 10^{16} \text{ s}^{-1}$.

As mentioned in [12], simulation based on Johnson and Christy's dielectric constant gives a blue shift, whereas simulation based on Palik's constant gives a very good fit of the experimental data obtained with nanoparticles of diameter 20.0 nm to 75.0 nm.

To introduce reduction of the mean free path of conduction electrons, the complex dielectric constant $\epsilon = \epsilon^- + i\epsilon''$ should be split into contribution of the bound (B_l and B_2) and free ($A_l(R)$ and $A_2(R)$) electrons [12]

$$\begin{aligned} \epsilon(R) &= (A_1(R) + B_1) + i(A_2(R) + B_2), \\ A_1(R) &= 1 - \frac{\omega_p^2}{\omega^2 + \omega_0(R)^2}, \\ A_2(R) &= \frac{\omega_p^2 \omega_0(R)^2}{\omega(\omega^2 + \omega_0(R)^2)}, \end{aligned}$$

Parameters B_l and B_2 represent contribution of bound electrons which are independent of particle size. They could be extracted from the complex dielectric constant of bulk silver

$$\hat{\epsilon} = (A_1 + B_1) + i(A_2 + B_2)$$

where A_1 and A_2 are solved as above, using the collision frequency and the dielectric constant of bulk silver, $\omega_0 = \frac{1}{\tau_s}$ and $\hat{\epsilon} = \epsilon + i\epsilon''$, accordingly.

Thus dielectric constant dependence of wavelength for silver nanoparticles is highly important data for the simulation. The real ϵ' and imaginary ϵ'' components of the dielectric constant ϵ could be found from the next equations:

$$\begin{aligned} \epsilon' &= n^2 + k^2 \\ \epsilon'' &= 2nk \end{aligned}$$

where n is the refractive index of silver, and k is the wave vector $k = 2\pi/\lambda$. In other words the complex refractive index $\hat{n} = n + ik$ and the complex dielectric constant $\hat{\epsilon} = \hat{n}^2$. Parameters n and k values of materials depend on the wavelength.

3 Silver Nanoparticle Synthesis: The Polyol Method

3.1 Literature Review

The polyol method involves suspending the metal precursor in a glycol solvent and subsequently heating the solution to a refluxing temperature. This technique has been used to synthesize metallic, oxide, and semiconductor nanoparticles. Often, a polyol is used as solvent, reducing agent, and ligand, to prevent NP agglomeration. The choice of polyol type is dictated by the optimum reflux temperature. Often, several hours of heating are required to produce NPs when convective heating is used. To extract the nanoparticles, after the reaction is completed, the solution is cooled to room temperature, and the silver particles are separated from the liquid by centrifugation and then repeatedly washed with ethanol. The resulting particles are dried at room temperature.

Apart from heating the reactant mixture, we can dissolve the capping agent in the solvent, heat it and then inject the silver precursor dissolved in the solvent into the heated mixture. In order to obtain monodisperse metal particles, generally, rapid nucleation in a short period of time is important; that is, almost all ionic species have to be reduced rapidly to metallic species simultaneously, followed by conversion to stable nuclei so as to be grown. The motivation behind this method was to overcome the challenge of gradual reduction of Ag^+ and nucleation of resultant Ag_0 by injecting Ag^+ in the heated EG+PVP mix. The size of the resulting silver particles was strongly dependent upon the reaction temperature (that of EG+PVP mix) and the injection rate.

Injecting the silver precursor generates a more monodisperse nanoparticle sample because upon addition of the silver nitrate aqueous solution to hot ethylene glycol, the Ag^+ species are reduced to metallic silver. The concentration of metallic silver in solution increases, reaching the supersaturation conditions and finally the critical concentration to nucleate. Spontaneous nucleation then takes place very rapidly and many nuclei are formed in a short time, lowering the silver concentration below the nucleation and supersaturation levels into the saturation concentration region. After a short period of nucleation, the nuclei grow by the deposition of metallic silver until the system reaches the saturation concentration. At the end of the growth period, all the metal particles have grown at almost the same rate and the system exhibits a narrow particle size distribution. [7].

Polymers are also used as capping agents to stabilize the nanoparticles and prevent agglomeration. It appears that when a small amount of PVP is used, agglomeration occurs as a result of incomplete covering of the silver particles with PVP [8]. Based on work by Dang *et al.* [8] when we increase PVP concentration, the nucleation rate of the silver particles is much higher and the particle size decreases until an optimum is reached at 3 mM. This implies that PVP can prevent as-synthesized Ag nanoparticles from aggregating, producing smaller particles and coordination through ester bond of PVP to the silver is expected due to electrostatic attraction. This tends to stabilize the silver nanoparticle and also keep nanoparticles small. Peak in FTIR absorbance spectra of PVP with and without silver nanoparticles suggests that PVP coordinates with silver nanoparticles by breakup of C=O double bond of the pyrrolidone groups. This coordination stabilizes the nanoparticle.

An interesting work by Wolf *et al.* [9] shows that it is possible to setup lab tabletop automated setup for synthesizing silver nanoparticles of sought size with high monodispersion through precise computed control of reaction conditions.

Another work by Lalegani *et al.* [10] showed that it is possible to significantly fasten the synthesis process by using Microwave assisted heating, which brought down the reaction duration by an order of magnitude without deteriorating the size distribution of the synthesized nanoparticles.

3.2 Our Synthesis

We used ethylene glycol (ethane-1,2-diol) as the solvent and reducing agent. For capping agent, we used Polyvinylpyrrolidone (C_6H_9NO)_n (PVP). For silver precursor, we used silver nitrate AgNO_3 .

Synthesis steps:

1. Dissolve the selected amount of PVP in ethylene glycol by constantly stirring it in a magnetic stirrer setup. Add PVP in small quantities at a time while dissolving to prevent lump formations.
2. Once PVP is dissolved, add the selected amount of silver nitrate.

3. Heat the mixture in a refluxer using an oil bath at 120 degree Celsius for 3 hours. While the boiling point of ethylene glycol is 195 degree Celsius, we operated at a lower temperature for stability of synthesized nanoparticles.

We prepared 6 samples:

AgNO ₃ (mg)	PVP (mg)	Ethylene Glycol (mL)
25	500	50
50	500	50
100	500	50
100	750	50
150	500	50
200	500	50

Following image shows the color contrast in the samples upon changing the silver nitrate concentration.

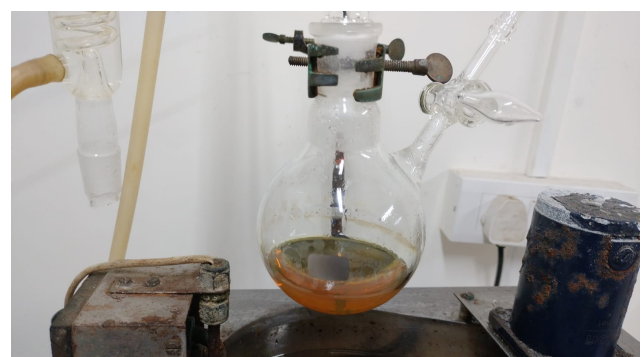


Figure 1: Color contrast from transparent to brown opaque as we increase the Silver nitrate from 25mg to 200mg

The following image shows the synthesis setup in the oil bath at the beginning and at the end of the reaction for 100mg AgNO₃ and 500mg PVP sample.



(a) Reaction flask in oil bath at t=0



(b) Reaction flask removed from oil bath after 3 hours

Figure 2: Synthesis setup in the oil bath at the beginning and at the end of the reaction for 100mg AgNO₃ and 500mg PVP sample.

4 Characterization Techniques and Observations

4.1 Transmission electron microscopy

TEMs employ a high voltage electron beam in order to create an image. An electron gun at the top of a TEM emits electrons that travel through the microscope's vacuum tube. Rather than having a glass lens focusing the light (as in the case of light microscopes), the TEM employs an electromagnetic lens which focuses the electrons into a very fine beam. This beam then passes through the specimen, which is very thin, and the electrons either scatter or hit a fluorescent screen at the bottom of the microscope. An image of the specimen with its assorted parts shown in different shades according to its density appears on the screen. This image can be then studied directly within the TEM or photographed.

We imaged two sample: 100mg AgNO₃ and 500mg PVP and 200mg AgNO₃ and 500mg PVP. We also performed an approximate size distribution analysis using ImageJ.

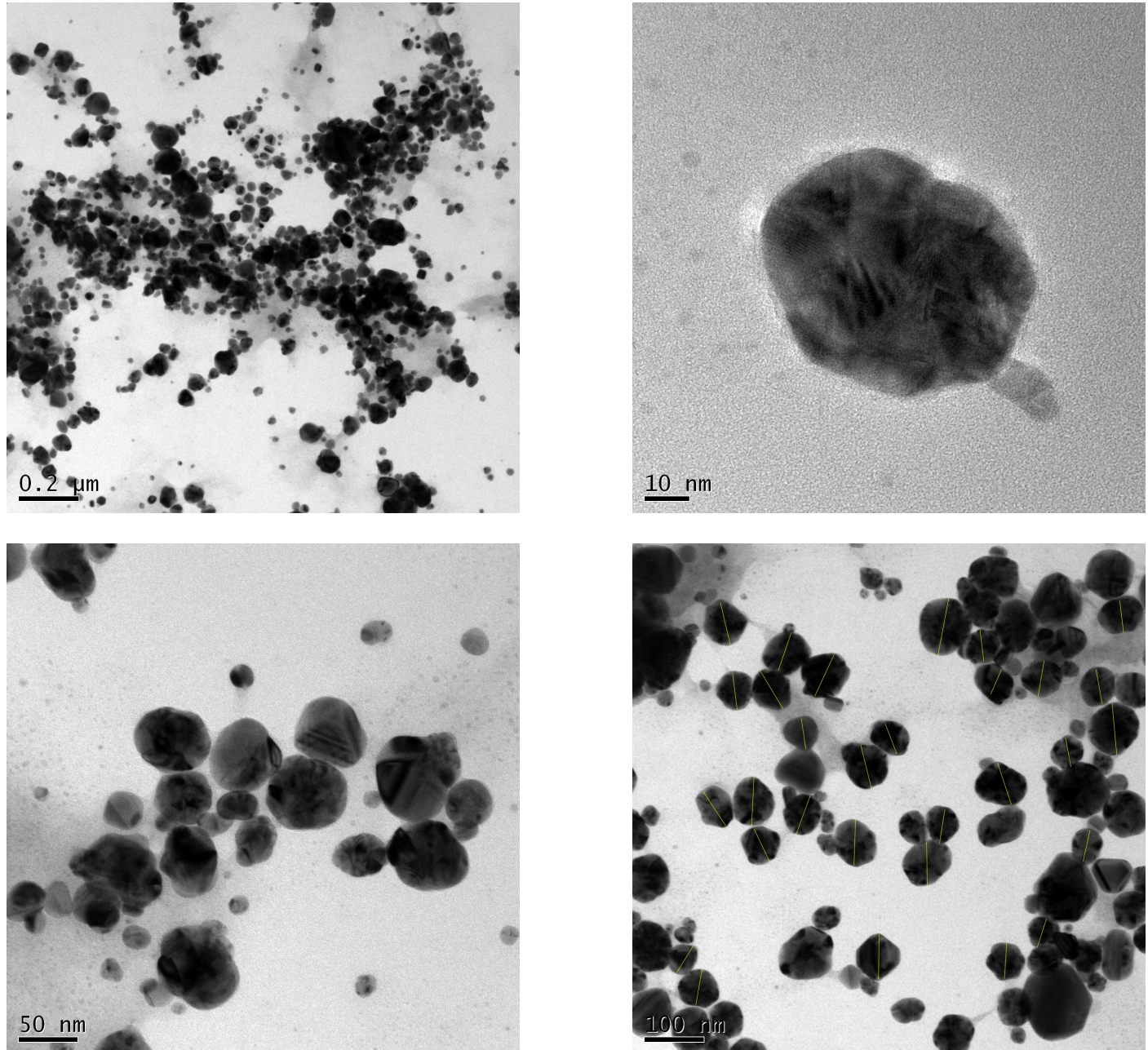


Figure 3: Images for 100mg AgNO₃ and 500mg PVP sample

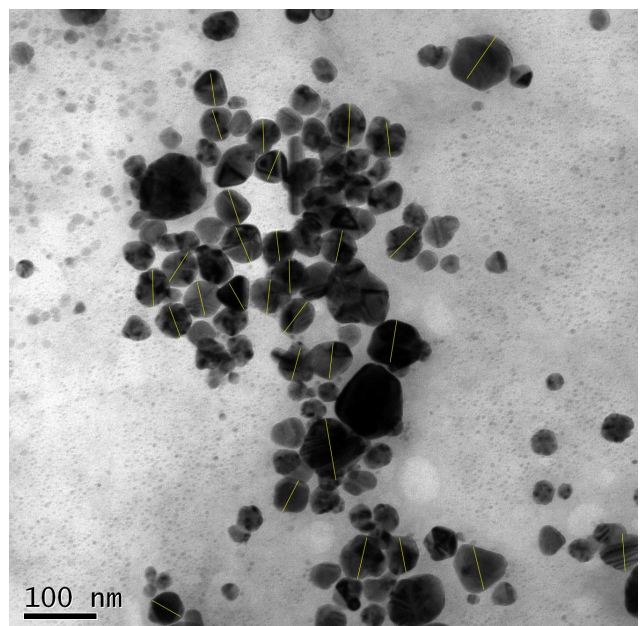
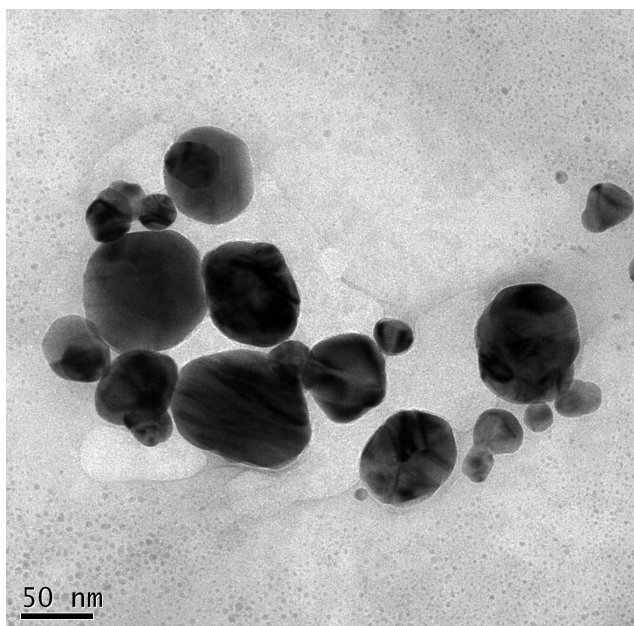
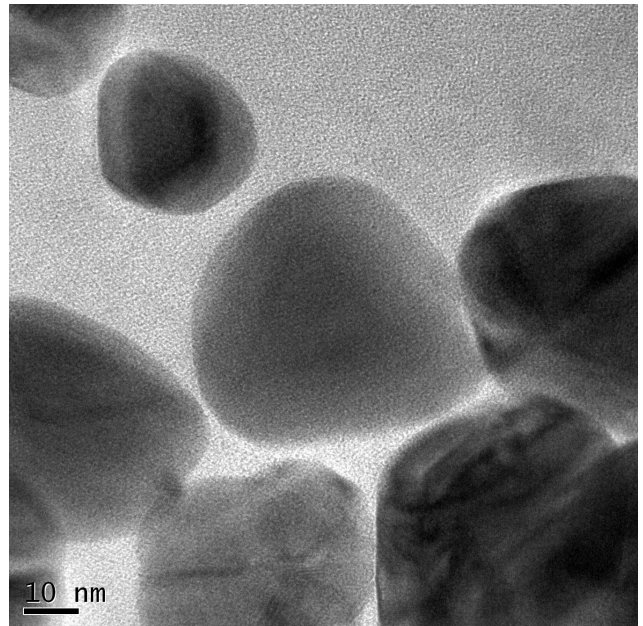
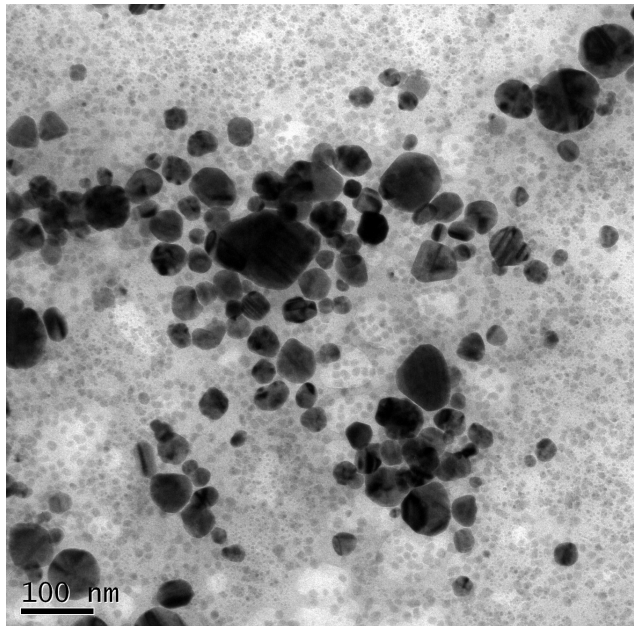
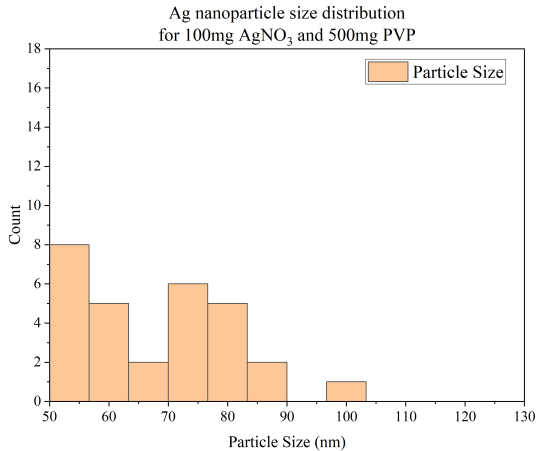


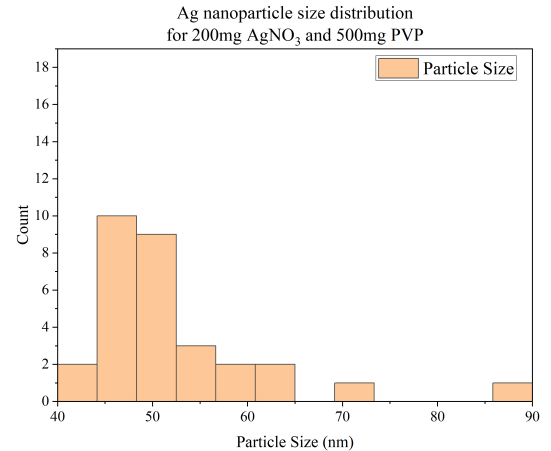
Figure 4: Images for 200mg AgNO_3 and 500mg PVP sample

4.1.1 Size Distribution of Ag particles

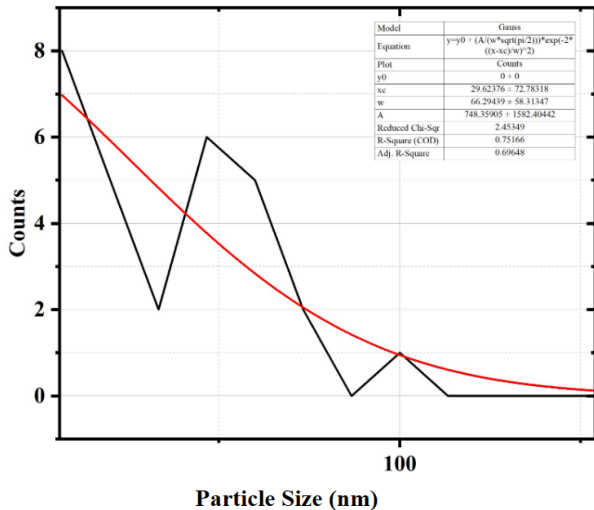
From the analysis done on the TEM images, we plotted the obtained sizes of particles. A Gaussian distribution is fitted across the bin centers to obtain the size distribution. The obtained distribution is then used to simulate the absorbance spectra applying Mie Theory in section 5. The small size of sample space and irregularities in shapes hinders us from capturing the correct size parameters.



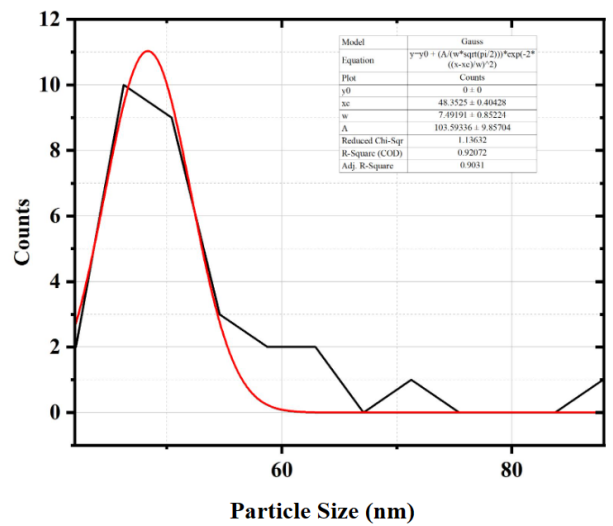
(a) Reciprocal space image for 100mg AgNO₃ and 500mg PVP sample



(b) Reciprocal space image for 200mg AgNO₃ and 500mg PVP sample



(c) Reciprocal space image for 100mg AgNO₃ and 500mg PVP sample

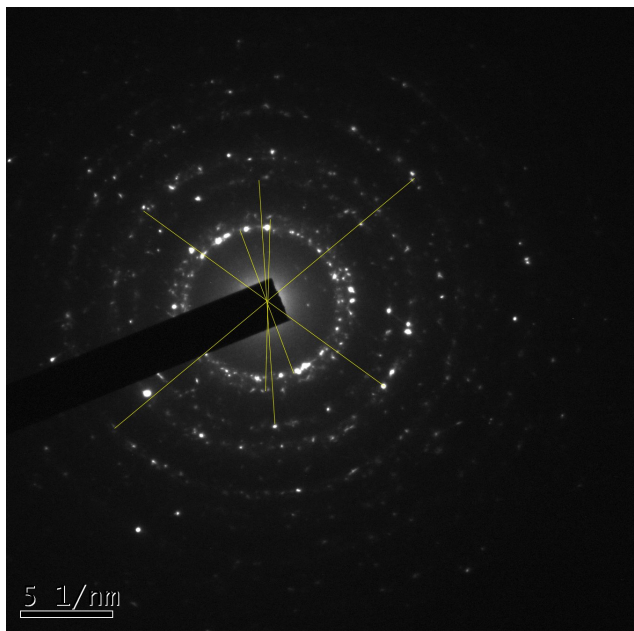


(d) Reciprocal space image for 200mg AgNO₃ and 500mg PVP sample

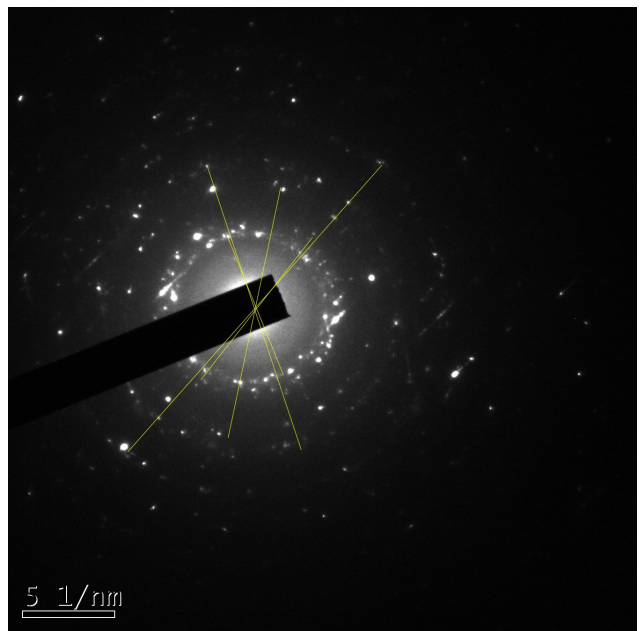
4.2 Selected area electron diffraction

Using the TEM setup, we can also perform diffraction study to evaluate the Miller indices of the planes present in the sample if it is of crystalline or polycrystalline nature. Like the standard diffraction study that used photons, for greater resolution due to smaller wavelength, we use an energetic electron beam. Since the beam exposure area is limited, hence selected area electron diffraction. Based on the Bragg's law and the selection rules of interference of beams reflected from crystal planes, we get certain spots in the k-space, which correspond to the Miller indices.

Since our sample was polycrystalline, we got rings in the k-space, because specific [hkl] planes were randomly oriented in space. Since silver crystallises in the cubic structure, the inverse of the distance of the rings from the centre, gave us the planar spacing. We then used the references from JCPDS, to map [hkl] to relevant distances.



(a) Reciprocal space image for 100mg AgNO_3 and 500mg PVP sample



(b) Reciprocal space image for 200mg AgNO_3 and 500mg PVP sample

Since the circles in the images were smudged, the assessment of $[\text{hkl}]$ from the distances was only an approximate calculation, based on JCPDS references.

Analysis for 100mg AgNO_3 and 500mg PVP sample

$2/d$ Reciprocal Space (nm^{-1})	d (Angstroms)	$[\text{hkl}]$	JCPDS Reference
8.117	2.464	111	00-001-1164
9.153	2.185	200	00-001-1164
13.028	1.535	220	00-001-1164
15.892	1.258	311	00-001-1164
20.838	0.960	331	00-001-1164

Analysis for 200mg AgNO_3 and 500mg PVP sample

$2/d$ Reciprocal Space (nm^{-1})	d (Angstroms)	$[\text{hkl}]$	JCPDS Reference
7.874	2.540	111	00-001-1164
9.652	2.072	200	00-001-1164
13.64	1.466	220	00-001-1164
15.906	1.257	311	00-001-1164
20.438	0.978	331	00-001-1164

4.3 UV-Vis Absorption Spectroscopy

Noble metals like gold and silver have non-zero absorbance in the UV region. The absorbance is related to the bandstructure of the noble metals, with the involvement of d-orbitals for the noble metals. For nanoparticles, the absorbance shows particle size effects, thus there is a shift in the peak corresponding to the particle size. Since the employed method produced particles of different sizes, the combined contribution of them produced the UV-Vis spectra presented in Fig(??).

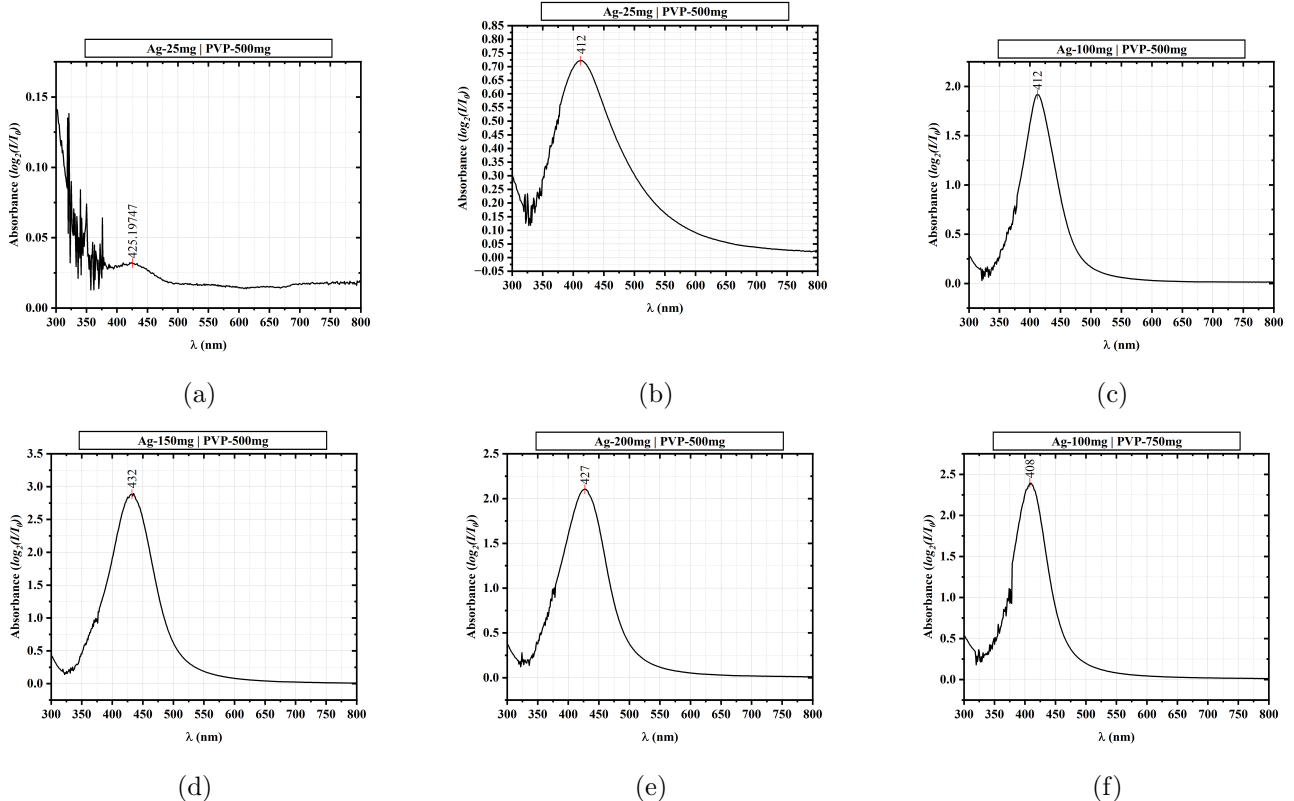


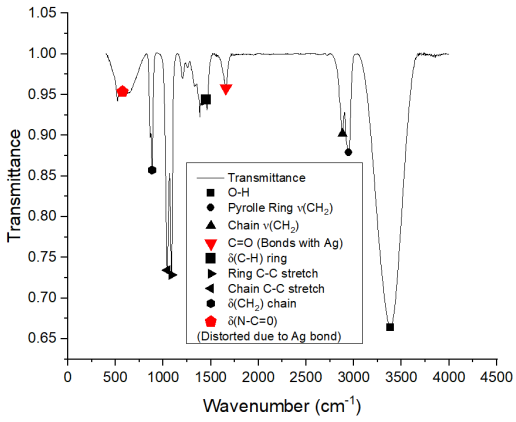
Figure 7: UV-Vis spectra for the 6 samples created with varying $AgNO_3$ and PVP concentrations. The corresponding concentrations are present on the images.

The shift in peak positions is indicative of the change in size distribution of Ag NPs. A blue shift can be recognised with increasing Ag concentration between 25mg and 200mg Ag with 500mg PVP. However the change is not monotonic, which can be attributed to the various shapes of Ag particles produced and the small dataset used to capture the size distribution.

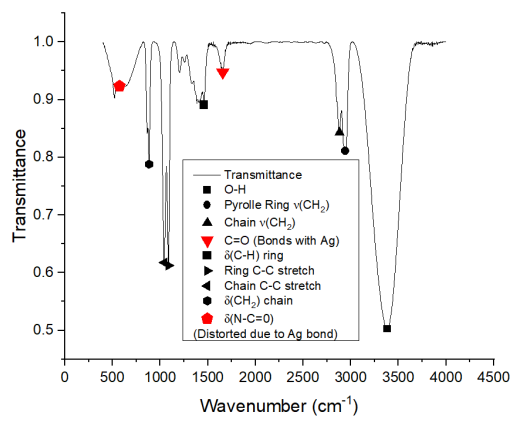
4.4 Fourier Transform Infrared Spectroscopy

FTIR [6] is uses the mid-range IR radiation to detect the vibrational energy levels characteristic to specific bonds in organic molecules. The advantage of Fourier transform comes from the fact that the entire wavelength range is scanned in a single shot using a unique type of signal which has all of the infrared frequencies superposed. The signal can be measured very quickly, usually on the order of one second or so. Thus, the time element per sample is reduced to a matter of a few seconds rather than several minutes. The resultant signal is then Fourier decomposed to get response at each frequency via the decomposition amplitude.

We measure the transmittance of the signal, so a dip indicates higher absorbance at that frequency, which correspond to the vibrational energy levels



(a) FTIR Spectrum for 100mg AgNO_3 and 500mg PVP sample



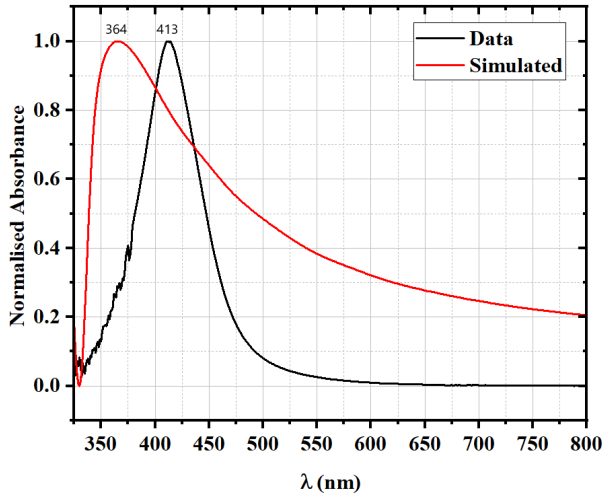
(b) FTIR Spectrum for 200mg AgNO_3 and 500mg PVP sample

The red-labeled peaks correspond to the bonds that participate in interaction with the Silver metal atoms. The peaks shifted and distorted due to metal interaction. Metal interacts with carbonyl ($\text{C}=\text{O}$) in the pyrrole ring. Therefore, $\text{C}=\text{O}$ and $\text{N}-\text{C}=\text{O}$ bonds are affected.

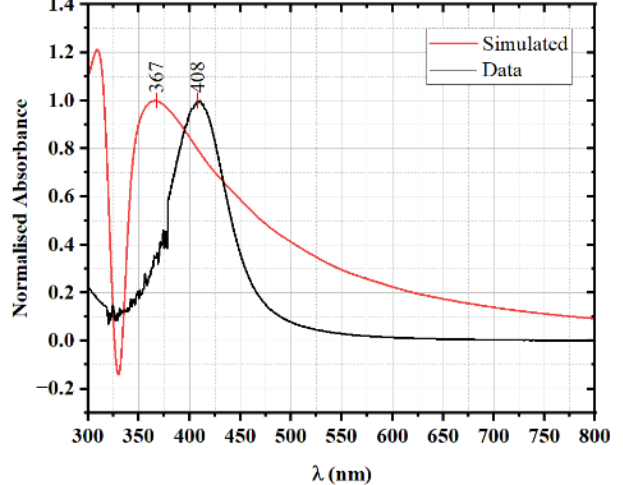
The transmittance at characteristic dips is lower for the 200mg AgNO_3 sample despite both samples having the same amount of PVP. This also indicates that PVP binds to metal atoms. More metal atoms in the 200mg case lead to more binding of PVP molecules to metal atoms. Hence, a possible explanation for a greater absorption.

5 Mie Theory Analysis

Following the method described in section 2 we performed simulations for the extinction coefficient for Ag nanoparticles. The simulations were performed with the bulk-Ag refractive index given by Johnson and Christy [1972] [11]. Reference [12] uses data provided by Palik[13], which gives more accurate results, however, we couldn't obtain the data, and thus stucked with 11.



(a) 100mg AgNO_3 and 500mg PVP



(b) 100 mg AgNO_3 and 750mg PVP

Figure 9: Simulated and Observed UV-Vis spectra

The peak shift with change in particle size distribution is captured well by the model, however, the position of peaks is blue shifted in the simulated data which is also reported in [11]. Thus, under the given model we are able to analyse the data well. A blue shift is observed with increasing particles size/ AgNO_3 concentration which fits well with the classical limit.

A different approach could be to fit the data with the size parameter. We did not follow that approach since

we obtained the size distribution from TEM. The effect of change in PVP concentration is clearly captured by the peak shifts.

6 Conclusion

Ag nanoparticles were obtained by the polyol method. SAED studies showed that the silver nanoparticles were polycrystalline with various plane directions of growth in a single particle.. The size evolution of their optical properties was evaluated with size distribution obtained from TEM images. FTIR was performed which provided conclusive results for the effect of PVP and silver nanoparticle bonding. The redshift and broadening of the surface plasmon band with a decrease in size is in agreement with the classical models. An increase in the Ag quantity can result in the damping of the surface plasmon band due to the dipolar interaction between the silver nanoparticles. It would be worthwhile to apply these models to such systems to gage the particle size range under which these composites exhibit SPR resonance bands.

Acknowledgement

We are thankful to Professor Aslam for providing us the opportunity to work on this project. We would also like to thank the Project TA, Bhawna Kalonia and Lab In-charge, Shripal Singh for their constant support and guidance throughout the project.

7 References

1. Wu, C.; Zhou, X.; Wei, J., Localized Surface Plasmon Resonance of Silver Nanotriangles Synthesized by a Versatile Solution Reaction. *Nanoscale Research Letters* 2015, 10 (1), 354.
2. Ghosh, S. K.; Pal, T., Interparticle Coupling Effect on the Surface Plasmon Resonance of Gold Nanoparticles: From Theory to Applications. *Chemical Reviews* 2007, 107 (11), 4797-4862.
3. Wiley, B.; Herricks, T.; Sun, Y.; Xia, Y., Polyol Synthesis of Silver Nanoparticles: Use of Chloride and Oxygen to Promote the Formation of Single-Crystal, Truncated Cubes and Tetrahedrons. *Nano Letters* 2004, 4 (9), 1733-1739.
4. Puspita, J. C.; Umar, A.; Imawan, C., Synthesis of silver nanoparticles using polyol method with the addition of hydrochloric acid as an additive. *AIP Conference Proceedings* 2022, 2391 (1), 050008.
5. Ashkarran, A. A.; Bayat, A., Surface plasmon resonance of metal nanostructures as a complementary technique for microscopic size measurement. *International Nano Letters* 2013, 3 (1), 50.
6. Johnson, G.J., 2005. Encyclopedia of Analytical Science. *Reference Reviews*, 19(8), pp.38-39.
7. Kim, D., Jeong, S. and Moon, J., 2006. Synthesis of silver nanoparticles using the polyol process and the influence of precursor injection. *Nanotechnology*, 17(16), p.4019.
8. Dang, T.M.D., Le, T.T.T., Fribourg-Blanc, E. and Dang, M.C., 2012. Influence of surfactant on the preparation of silver nanoparticles by polyol method. *Advances in natural sciences: nanoscience and nanotechnology*, 3(3), p.035004.
9. Wolf, J.B., Stawski, T.M., Smales, G.J., Thünemann, A.F. and Emmerling, F., 2022. Towards automation of the polyol process for the synthesis of silver nanoparticles. *Scientific Reports*, 12(1), p.5769.
10. Lalegani, Z., Ebrahimi, S.S., Hamawandi, B., La Spada, L. and Toprak, M.S., 2020. Modeling, design, and synthesis of gram-scale monodispersed silver nanoparticles using microwave-assisted polyol process for metamaterial applications. *Optical Materials*, 108, p.110381.
11. P.B. Johnson, R.W. Christy, Optical constants of the noble metals, *Phys. Rev. B* 6 (1972) 4370–4379, <https://doi.org/10.1103/PhysRevB.6.4370>.
12. D. Paramelle , A. Sadovoy , S. Gorelik , P. Free , J. Hobley and D. G. Fernig , *Analyst*, 2014, 139 , 4855 –4861
13. Edward D. Palik, *Handbook of Optical Constants of Solids*, Academic Press, 1997

14. Wilcoxon J P, Martin J E and Porencio P 2001 *J. Chem. Phys.* 115 998
15. Smithard M A and Dupree R 1972 *Phys. Status Solidi a* 11 695
16. Mandal S K, Roy R K and Pal A K 2002 *J. Phys. D: Appl. Phys.* 35 2198
17. Bohren C F and Huffman R R 1998 *Absorption and Scattering of Light by Small Particles* (New York: Wiley-Interscience) p 337